

Surface Diffusion: The Low Activation Energy Path for Nanotube Growth

S. Hofmann,¹ G. Csányi,² A. C. Ferrari,^{1,*} M. C. Payne,² and J. Robertson¹

¹Department of Engineering, University of Cambridge, Cambridge CB2 1PZ, United Kingdom

²Cavendish Laboratory, University of Cambridge, Cambridge CB3 0HE, United Kingdom

(Received 25 January 2005; published 12 July 2005)

We present the temperature dependence of the growth rate of carbon nanofibers by plasma-enhanced chemical vapor deposition with Ni, Co, and Fe catalysts. We extrapolate a common low activation energy of 0.23–0.4 eV, much lower than for thermal deposition. The carbon diffusion on the catalyst surface and the stability of the precursor molecules, C₂H₂ or CH₄, are investigated by *ab initio* plane wave density functional calculations. We find a low activation energy of 0.4 eV for carbon surface diffusion on Ni and Co (111) planes, much lower than for bulk diffusion. The energy barrier for C₂H₂ and CH₄ dissociation is at least 1.3 eV and 0.9 eV, respectively, on Ni(111) planes or step edges. Hence, the rate-limiting step for plasma-enhanced growth is carbon diffusion on the catalyst surface, while an extra barrier is present for thermal growth due to gas decomposition.

DOI: 10.1103/PhysRevLett.95.036101

PACS numbers: 81.16.Hc, 61.46.+w, 81.07.-b, 81.10.Aj

The controlled synthesis of nanoscale materials such as carbon nanotubes (CNTs) and carbon nanofibers (CNFs) is a fundamental step for the bottom-up fabrication of devices [1]. Many growth studies focus on surface-bound chemical vapor deposition (CVD) [2,3], which uses pre patterning of catalysts for selective growth. This has led to considerable effort to understand the catalytic growth process [4,5], with the ultimate aim of controlling the CNT properties and boosting their yield [6]. So far, the growth process has been optimized empirically, because the catalyst interaction with the carbon precursors is not fully understood. Previous theoretical studies mainly focused on nucleation [5,7,8]; however, a key factor is the kinetics of carbon supply. Although the dissociative adsorption of hydrocarbons on a metal surface is central to heterogeneous catalysis in general [9], little attention has been paid to this crucial step in the context of CNT or CNF growth. For surface-bound CVD, there is an application-driven need for low growth temperatures to enable the use of more sensitive substrates or integration processes. Low temperature could also allow a more deterministic growth, reducing the number of competing microscopic processes. However, little effort has been devoted so far to determine the onset of growth at low temperatures.

Thermal CVD is characterized by an activation energy of ~1.2–1.8 eV [10–13]. Low growth temperatures were reported with plasma-enhanced CVD (PECVD) [2,14–16], with a lower activation energy of ~0.3 eV [2]. To understand these activation energies, we need to consider the fundamental processes in CNT or CNF CVD during tip or base growth: (1) adsorption of the gas precursor molecule on the catalyst surface, (2) dissociation of the precursor molecule, (3) diffusion of the growth species in or on the catalyst particle, and (4) nucleation and incorporation of carbon into the growing structure [Fig. 1(a)].

In this Letter, we consider the individual energy barriers for processes (1)–(4), to identify the rate-limiting step. As the processes are sequential, the rate-limiting step in a

proposed reaction path corresponds to the slowest process with the largest energy barrier. We also exclude reaction paths which require higher barriers than experimentally observed. We measure activation energies of 0.2–0.4 eV for surface-bound PECVD of CNFs with the most common catalysts (Ni, Co, and Fe), much lower than for thermal deposition. We then investigate carbon diffusion on the catalyst surface and the stability of the precursor gases (C₂H₂ or CH₄) by first-principles calculations. We find a low activation energy for surface diffusion on Ni and Co (111) planes. The barrier for C₂H₂ or CH₄ dissociation on the catalyst interface exceeds 0.9 eV on Ni(111) planes or edges. Therefore, we propose that the limiting step for plasma-enhanced synthesis is carbon diffusion on the catalyst surface. On the contrary, the activation energy for thermal growth has to be at least as high as the barrier for gas decomposition.

In the commonly accepted growth mechanism, carbon dissolves into the catalyst and CNTs or CNFs grow by precipitation of excess carbon on the metal surface above or behind the catalyst particle [4,5,10]. This idea originates from the vapor-liquid-solid (VLS) mechanism suggested

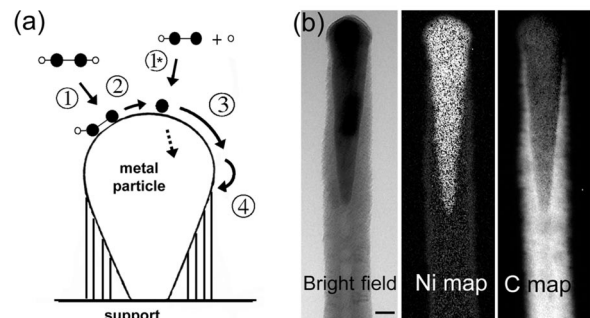


FIG. 1. (a) Schematic of the growth process. (b) Bright field image and electron energy loss spectroscopy Ni *L* edge (854 eV) and carbon *K* edge (284 eV) elemental maps of a PECVD CNF at 500 °C. Scale bar: 20 nm.

for solid silicon whiskers growth [17]. In this model, the catalyst forms a liquid droplet and preferentially adsorbs the growth species from the surrounding vapor. The solid whisker grows from this supersaturated eutectic liquid. However, CNF and single-wall CNT growth are reported at temperatures lower than 300 °C [2,15] and 600 °C [16,18], respectively, well below the (size-corrected) metal-carbon eutectic temperature [19]. This implies that the catalyst can be solid, in contrast to VLS. Furthermore, *in situ* transmission electron microscopy shows that the Ni catalyst stays crystalline throughout the thermal growth of CNFs at 540 °C [20]. Lattice-resolved images show neither carbide formation [21] nor extended liquid surface layers [22]. Baker and Harris [10] derived activation energies for CNF growth with Fe, Co, and Ni, and noted their similarity to those for C diffusion in the bulk metals. They thus suggested that the rate-limiting step for CNF growth is bulk C diffusion. However, recent calculations [20] argue that the thermal CVD energy barrier is a sum of activation energies of successive surface and step-edge processes, and is not due to bulk diffusion. This would imply the same high barrier for PECVD, in contrast with our measurements.

We perform a systematic study using Ni, Co, and Fe catalysts. Thin Ni films (~ 6 nm) are magnetron sputtered, and ~ 5 – 15 nm Co and Fe films are thermally evaporated onto oxidized Si(100) at base pressures below 10^{-6} mbar. Aligned CNFs [Fig. 1(b)] are grown using a dc PECVD system from a gas mixture of C_2H_2 (50 sccm) and NH_3 (200 sccm) at 0.7 mbar pressure. The detailed growth conditions are reported elsewhere [2]. Here we stress that the discharge current at 600 V does not exceed ~ 30 mA, and the power is less than ~ 20 W. This minimizes additional plasma heating to less than 40 °C, unlike high power depositions [14,23] where plasma heating significantly raises the substrate temperature [14,23].

Figure 2 compares the growth rate as a function of temperature for the different catalysts. In order to get accurate growth rate measurements, we prepattern the catalyst by e-beam lithography to get free standing vertically aligned CNFs [2], rather than rely on weight gain measurements [24] or unpatterned samples height [11–13]. In the 250–500 °C range, the Ni and Co growth rates are very similar, whereas for Fe it is lower. Nevertheless, it is clear that the activation energy is always below 0.4 eV.

First-principles calculations of the reaction paths are done with the CASTEP plane wave density functional theory code [25] on slab models of the catalyst-carbon system. We use the Perdew-Burke-Ernzerhof gradient corrected functional and ultrasoft pseudopotentials with a 360 eV energy cutoff. Spin polarization is included, and the Brillouin zone is sampled by a $3 \times 3 \times 1$ mesh. We use 5 and 4 layer slabs of metal to represent the (111) and (100) surfaces, respectively, and always keep the atomic positions in the bottom layer fixed. The vacuum layer between slabs is at least 5 Å, and, unless otherwise stated, the surface supercell is 2×2 . We compute the relative energies of a number of meta-

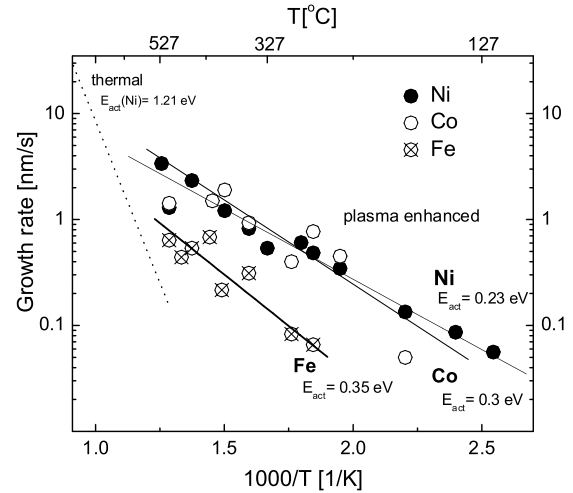


FIG. 2. Arrhenius plots for CNF growth rates on different catalysts in NH_3 diluted C_2H_2 . The activation energies are calculated from the slope of the linear fit to the data. Temperature dependent changes in the CNFs crystallinity are not considered. The dotted line is the growth rate variation for Ni thermal CVD ($E_{act} = 1.21$ eV [11,42]).

stable configurations and the lowest energy transition states (TSs) between them. We then examine the most likely reaction pathways, and evaluate the highest calculated energy barrier between the initial and final states. In each case, the TS is identified by selecting a reaction coordinate (usually the distance between two atoms, e.g., C-H, or C metal), and locating the highest energy configuration along the reaction path after geometry optimization, keeping a fixed value of the reaction coordinate. Although this is not an exhaustive procedure, we emphasize here that the crucial point is the *existence* of low barrier pathways. In the case of surface diffusion, the high symmetry of the system gives confidence that our barrier is the lowest possible. Should a diffusion path later be found with an even lower barrier, it would only strengthen our conclusions.

Recall the four sequential steps of growth shown in Fig. 1(a): (1) precursor adsorption, (2) dissociation, (3) C transport, and (4) C incorporation. There is a driving force for graphene formation due to the energy gain per incorporated C atom [20,26]. Independent of the initial nucleation mechanism, the barrier for process (4) is small, because no covalent bonds are being broken. We verify this by taking the geometry-optimized configuration of a graphene sheet (represented by a thin strip) lying on a Ni (111) surface, and placing an additional C atom at a nearby hollow site [Fig. 3(a)]. The surface unit cell is 4×2 ; we include 3 metal layers and fix the positions of Ni atoms in the lowest layer as well as of the C atoms at one edge of the strip. Upon relaxation, the additional C atom spontaneously joins the existing graphitic structure.

Carbon transport and incorporation into CNT walls are unlikely to be very different for thermal and plasma CVDs, so the role of plasma must be in processes (1) and (2).

Neglecting self-pyrolysis, in thermal CVD, hydrocarbon dissociation occurs on the catalyst surface [20,27]. Similar reactions are involved in many catalytic processes such as hydrogenation or steam reforming. The adsorption (1) and dissociation (2) steps [Fig. 1(a)] of C_2H_2 and CH_4 on low index metal surfaces are different. On Ni(111), C_2H_2 adsorbs exothermically (with 2.9 eV adsorption energy [28]) without dissociation, whereas CH_4 can adsorb only on the Ni surface via dissociative adsorption. This gives a sticking coefficient at zero coverage for C_2H_2 of ~ 1 compared to $\sim 10^{-7}$ for CH_4 [29]. This explains why C_2H_2 is often a more effective precursor than CH_4 . On the other hand, C_2H_2 is more likely to block reactive sites due to a higher saturation coverage [30].

Thus, we must calculate the dissociation energy for both C_2H_2 and CH_4 . We do this for the most stable Ni surface: (111) [31,32]. We find a barrier of ~ 1.4 eV for dissociation by the H abstraction reaction $C_2H_2 \rightarrow C_2H + H$ on Ni(111) [Fig. 3(b)]. For comparison, the dissociation energy for an isolated C_2H_2 molecule in vacuum is 5.58 eV [33], underlining the catalytic effect. We also include the possible role of step edges in the reaction, since it was proposed that these may lower the barrier [26]. We thus consider a stepped Ni(111) surface. We find a barrier of 1.3 eV for C_2H_2 dissociation [Fig. 3(c)]. The binding energy of C_2H_2 at the step is 0.7 eV higher than adsorption on the flat surface. Thus the step edge *does not* help significantly the C_2H_2 dissociation. For CH_4 on Ni(111), we calculate the barrier for the dissociative adsorption taking the transition state from [34]. We obtain a barrier of 1.2 eV, consistent with [34], whereas on the step edge the barrier is 0.9 eV [26]. However, this barrier is still significant and should not be ignored as done in [20]. Summarizing, the *minimum* energy barriers for C_2H_2 and CH_4 in processes (1) and (2) for thermal CVD are 1.3 eV and 0.9 eV, respectively. Thus, the minimum barrier for thermal CVD is H abstraction, and the overall activation energy must be equal to or larger than the dissociation barrier, in agreement with experiments [10–13].

In PECVD, the plasma creates new and more reactive species, such as radicals, in the gas phase and/or the catalyst surface [35–37]. This allows a reduction of the growth activation energy, as, e.g., atomic carbon can chemisorb directly on the catalyst [38,39]. The adsorption of higher molecular species can change significantly in a plasma. Dissociative chemisorption can be induced by collisions [40], particularly in dc plasmas. The sticking coefficient at zero coverage is found to vary with the different forms of excitation energies in the reaction, increasing drastically for vibrational excitation of CH_4 [41]. The higher amount of carbon radicals in a plasma manifests itself as noncatalytic amorphous carbon deposition [37]. Indeed, diluents and etchants are needed in PECVD to create reactive species etching the catalyst surface, in order to keep the surface transport paths open [2,42]. The key role of diluents was recently shown also for thermal CVD [6]. In general, the surface chemistry is much more

complex for plasma growth, and provides a richer carbon supply [35], schematically indicated as 1^* in Fig. 1(a). We therefore assume a negligible barrier for steps (1) and (2) in plasma growth. As there is no barrier for step (4), the energy barrier is then C diffusion [step (3)].

We find that the stable C absorption site on the Ni(111) surface is the hollow site, where C is bonded to 3 Ni atoms. The TS is a pass site, where C is bonded to two Ni [Fig. 3(d)]. The barrier for C diffusion on the Ni(111)

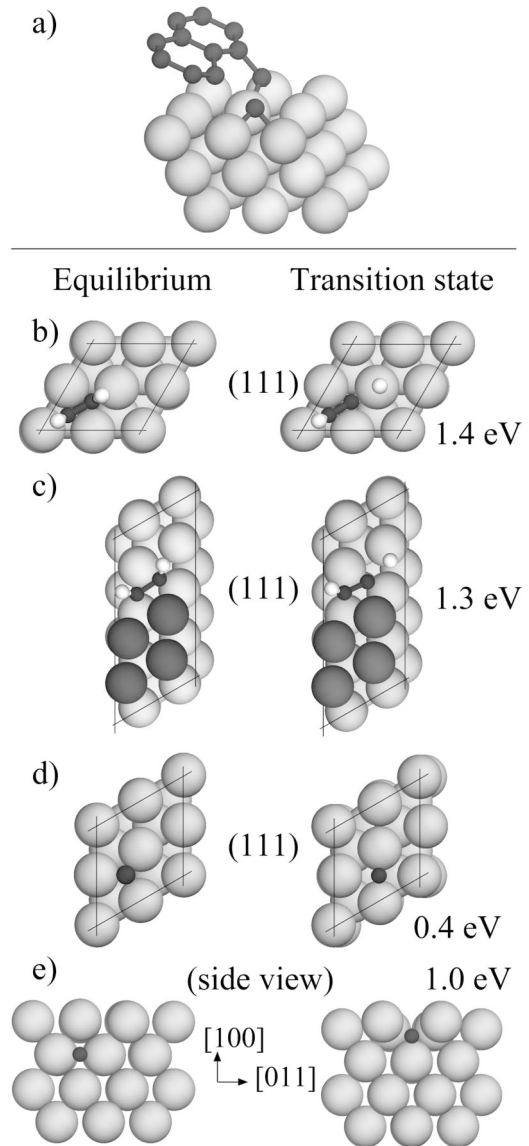


FIG. 3. (a) The incorporation of a new C atom into an existing graphene sheet on a Ni(111) surface proceeds spontaneously when started from this configuration, with the additional C atom placed at a nearby hollow site; (b)–(e) Equilibrium (left) and transition state (right) geometries: dissociation of C_2H_2 on (b) the Ni(111) surface; (c) Ni(111) step edge, where the large dark spheres indicate metal atoms of the topmost layer; (d) diffusion of a C atom on Ni(111) surface; (e) a subsurface pathway one layer below the Ni(100) surface. The transition barrier height is shown next to each TS geometry.

surface is 0.4 eV for this state. The barrier for C diffusion along the graphene-Ni(111) interface was found to be 0.5 eV [20], indicating that the C diffusion energy does not change significantly on formation of CNF or CNT walls. We get a similar barrier of 0.5 eV for a free Co(111) surface. On Ni(110), there is a similar barrier ~ 0.4 eV [32]. These are in good agreement with our data in Fig. 2.

We also investigate possible diffusion on Ni(100), which is energetically much less favored than (111). Here the atom corrugation is much deeper, and adsorbed C atoms are bonded to 5 Ni, but are farther away. C diffusion is more difficult. The barrier is 1.9 eV. However, even in this case, a lower energy path exists for *subsurface* diffusion [Fig. 3(e)] with an ~ 1.0 eV barrier. C migrates one layer below the surface. This lower barrier can be understood noting that the number of Ni-C bonds that have to be simultaneously broken is less than on the surface. Subsurface diffusion is still easier than deep inside the bulk, because Ni atoms just above the C atom can displace upwards to the surface, unlike in the bulk. Finally, the energy barrier for bulk diffusion of C in fcc Ni is ~ 1.6 eV [43]. As this exceeds that for $\text{CH}_4/\text{C}_2\text{H}_2$ dissociation, it is the rate-limiting step for CVD if surface diffusion on the catalyst is blocked by high carbon coverage.

In conclusion, the low activation energy for PECVD is due to surface diffusion. In contrast, the activation energy for thermal CVD has to be at least equal to the precursor molecules dissociation barrier. Maximizing catalyst activity and growth rate, thermal CVD of CNTs or CNFs should be possible at low temperatures via surface diffusion, as in PECVD. For bulk diffusion to operate as well, a higher energy barrier of ~ 1.6 eV needs to be overcome. Above the (size-corrected) eutectic temperature, a liquid catalyst could significantly influence the growth dynamics. Our conclusions are not restricted to CNTs or CNFs, but have implications for catalyst assisted growth of nanomaterials in general. Given an appropriate precursor supply, the growth can proceed via diffusion on a solid particle at low temperature. Indeed, it was recently shown that ZnSe and GaAs nanowires can grow below the eutectic temperature by using atomic beams [44,45].

Computations were carried out on CCHPCF, Cambridge, and on HPCx. This work was supported by EPSRC Grants No. GR/S61263 and No. GR/S97613 and by the EU project Cardecom. A. C. F. acknowledges funding by The Royal Society. S. H. acknowledges support from Peterhouse. We thank R. E. Dunin-Borkowski for EELS, B. Kleinsorge, C. Ducati, and G. Held for helpful discussions.

*Electronic address: acf26@eng.cam.ac.uk

- [1] R. H. Baughman *et al.*, *Science* **297**, 787 (2002).
- [2] S. Hofmann *et al.*, *Appl. Phys. Lett.* **83**, 135 (2003); **83**, 4661 (2003).
- [3] H. Cui *et al.*, *Appl. Phys. Lett.* **84**, 4077 (2004).
- [4] H. Kanzow and A. Ding, *Phys. Rev. B* **60**, 11 180 (1999).
- [5] J. Gavillet *et al.*, *Phys. Rev. Lett.* **87**, 275504 (2001).
- [6] K. Hata *et al.*, *Science* **306**, 1362 (2004).
- [7] X. Fan *et al.*, *Phys. Rev. Lett.* **90**, 145501 (2003).
- [8] V. L. Kuznetsov *et al.*, *Phys. Rev. B* **64**, 235401 (2001).
- [9] J. R. Anderson and M. Boudart, *Catalysis: Science and Technology* (Springer, Berlin, 1984), Vol. 5.
- [10] R. T. K. Baker and P. S. Harris, in *Chemistry and Physics of Carbon* (Marcel Dekker, New York, 1978), Vol. 14, p. 83.
- [11] C. Ducati *et al.*, *J. Appl. Phys.* **92**, 3299 (2002).
- [12] Y. T. Lee *et al.*, *J. Phys. Chem. B* **106**, 7614 (2002).
- [13] D. B. Geohegan *et al.*, *Appl. Phys. Lett.* **83**, 1851 (2003).
- [14] B. O. Boskovic *et al.*, *Nat. Mater.* **1**, 165 (2002).
- [15] M. Chen *et al.*, *Jpn. J. Appl. Phys.* **42**, 614 (2003).
- [16] Y. Li *et al.*, *Nano Lett.* **4**, 317 (2004).
- [17] R. S. Wagner and W. C. Ellis, *Appl. Phys. Lett.* **4**, 89 (1964).
- [18] R. Seidel *et al.*, *J. Phys. Chem. B* **108**, 1888 (2004).
- [19] Y. Qi *et al.*, *J. Chem. Phys.* **115**, 385 (2001).
- [20] S. Helveg *et al.*, *Nature (London)* **427**, 426 (2004).
- [21] I. Alstrup, *J. Catal.* **109**, 241 (1988).
- [22] F. Larouche *et al.*, cond-mat/0411675.
- [23] K. B. K. Teo *et al.*, *Nano Lett.* **4**, 921 (2004).
- [24] L. S. Lobo and D. L. Trimm, *Nature (London)* **234**, 15 (1971).
- [25] M. D. Segall *et al.*, *J. Phys. Condens. Matter* **14**, 2717 (2002).
- [26] H. S. Bengaard *et al.*, *J. Catal.* **209**, 365 (2002).
- [27] S. Fan, L. Liu, and M. Liu, *Nanotechnology* **14**, 1118 (2003).
- [28] J. W. Medlin *et al.*, *J. Phys. Chem. B* **107**, 217 (2003).
- [29] T. P. Beebe *et al.*, *J. Chem. Phys.* **87**, 2305 (1987).
- [30] L. Vattuone *et al.*, *Surf. Sci.* **447**, 1 (2000).
- [31] H. Leidheiser *et al.*, *J. Am. Chem. Soc.* **70**, 1206 (1948).
- [32] S. Hong *et al.*, *Jpn. J. Appl. Phys.* **41**, 6142 (2002).
- [33] G. D. Lee *et al.*, *Phys. Rev. B* **66**, 081403(R) (2002).
- [34] P. Kratzer *et al.*, *J. Chem. Phys.* **105**, 5595 (1996).
- [35] D. Hash *et al.*, *J. Appl. Phys.* **93**, 6284 (2003).
- [36] M. A. Liebermann and A. J. Lichtenberg, *Principles of Plasma Discharges and Materials Processing* (Wiley, New York, 1994).
- [37] A. von Keudell, *Thin Solid Films* **402**, 1 (2002).
- [38] D. J. Klinke *et al.*, *J. Catal.* **178**, 540 (1998).
- [39] Q. M. Zhang *et al.*, *Phys. Rev. B* **69**, 205413 (2004).
- [40] J. D. Beckerle *et al.*, *J. Chem. Phys.* **86**, 7236 (1987).
- [41] R. R. Smith *et al.*, *Science* **304**, 992 (2004).
- [42] M. Chhowalla *et al.*, *J. Appl. Phys.* **90**, 5308 (2001).
- [43] D. J. Siegel *et al.*, *Phys. Rev. B* **68**, 094105 (2003).
- [44] A. Colli *et al.*, *Appl. Phys. Lett.* **86**, 153103 (2005).
- [45] A. I. Persson *et al.*, *Nat. Mater.* **3**, 677 (2004).